IEEE Access
Multidisciplinary | Rapid Review | Open Access Journal

Received September 5, 2019, accepted September 19, 2019, date of publication September 30, 2019,
date of current version October 16, 2019.

Digital Object Identifier 10.1109/ACCESS.2019.2944462

Flexible Wideband Microstrip-Slotline-Microstrip Power Divider and Its Application to Antenna Array

BING XIAO[1], HEMING YAO[1], MIN LI[1], (Member, IEEE), JING-SONG HONG[2], AND KWAN L. YEUNG[1], (Senior Member, IEEE)

[1]Department of Electrical and Electronic Engineering, The University of Hong Kong, Hong Kong
[2]Institute of Applied Physics, University of Electronic Science and Technology of China, Chengdu 610054, China

Corresponding author: Min Li (minli@eee.hku.hk)

ABSTRACT In the satellite microwave power transmission (MPT) system, antenna arrays are usually adopted for a higher gain. For the passive wideband antenna array, wideband power dividers are essential when the feed network is constructed. Because the microstrip-slotline coupled power divider could achieve wide bandwidth and compact size at the same time, it becomes a potential candidate for the feed network. However, impedance matching is always needed in the slotline, e.g., the fixed slotline length or the stepped impedance transformation. So, the power divider is not flexible. In this paper, a flexible Microstrip-Slotline-Microstrip (MSM) power divider is presented. When the ratio of the coupling coefficients n_1 of the microstrip-to-slotline transition (MST) and n_2 of the slotline-to-microstrip transitions (SMT) is 2, the MST and SMTs could be self-matched respectively. Then no impedance matching is needed anymore in the slotline. Thus, the slotline length can be arbitrarily chosen, and no stepped impedance transformations are needed. This power divider eliminates the drawback limiting the free wire routing for the microstrip-slotline coupled feed network. It could serve as a new kind of feed network, especially be considered when the simple T-junction feed network cannot achieve enough bandwidth. Besides, a wideband Vivaldi array with this feed network is presented.

INDEX TERMS Feed network, microstrip-slotline coupling, wideband power divider, wideband antenna array.

I. INTRODUCTION

Satellite microwave power transmission (MPT) is a technology for distant power transfer in space [1]. To increase the transmission distance, Vivaldi antenna arrays could be adopted for higher gains. Vivaldi antenna element could easily achieve very wide bandwidth [2], [3]. However, in many situations with Vivaldi arrays, the bandwidth of the feed network becomes the bottleneck of the bandwidth of the array. Besides, satellite-borne RF components should be compact and lightweight. Based on the above two reasons, a planar feed network with small size and enough bandwidth is necessary. In the existing literature, the planar power dividers used in antenna array feed networks can be categorized as follows:

The first type is the cascaded impedance-matching T-junction. It has a simple and compact structure, so is widely used in antenna arrays. However, the simple T-junctions cannot achieve wide bandwidth, usually much narrower than one octave. So, they are usually used in narrowband antenna arrays [4]–[8]. In [7], stripline T-junctions are used to feed a 4-element Vivaldi array, achieving 9.7% bandwidth from 59 to 65 GHz.

The other type is the multisection Wilkinson power divider. It can achieve wide bandwidth and high isolation [9]–[13]. In [12], the three-section Wilkinson power divider is used to feed a 16-element Vivaldi array, achieving a 40% bandwidth from 8 to 12 GHz. In [13], the three-section Wilkinson power divider is used to feed an 8-element Vivaldi array, achieving a 147% bandwidth from 1.6–10.5 GHz. But it is bulky in the longitudinal direction due to the multisectional structure. The key indicators of the above Vivaldi arrays are compared in Table 1.

In addition to the above-mentioned two kinds of power dividers, the microstrip-slotline coupled power divider is also

The associate editor coordinating the review of this manuscript and approving it for publication was Lu Guo.

TABLE 1. Vivaldi arrays with different types of feed network.

	Feed network type	Element number	Frequency range (GHz)	Fractional bandwidth
[7]	Stripline T-junctions	4	59 - 65	9.7%
[12]	3-section Wilkinson	16	8 - 12	40%
[13]	3-section Wilkinson	8	1.6 - 10.5	147%
Proposed	Microstrip-slotline coupled	4	3.4 - 8.3	83.8%

TABLE 2. MSM four-way power dividers.

	Flexible	Frequency range (GHz)	Fractional bandwidth	Average insertion loss (dB)
[22]	X	3.7 - 10.1	92.8%	6.8
[23]	X	3.1 - 10.6	109.5%	8
Proposed	✓	4.3 - 8.1	61.3%	7 and 7.5

a candidate for the feed network. It could achieve wide bandwidth while keeping compact. Some power dividers of this kind were proposed by utilizing the wideband property of microstrip-slotline coupling [14]–[18]. The microstrip-slotline coupled structure is also utilized in [10], [19]–[21] to improve the bandwidth of Wilkinson power dividers. Furthermore, microstrip-slotline-microstrip (MSM) four-way power dividers [22], [23] were also proposed, as shown and compared in Table 2. They could be the origins of the research of the microstrip-slotline feed network.

However, these MSM power dividers have drawbacks limiting the free wire routing of the feed network. The lengths of the slotlines in these power dividers should be specifically fixed for impedance matching, e.g., a quarter guided wavelength [10], [15], half guided wavelength [14], or others [22], [23]. Otherwise, step impedance transformations should be used in the slotline [16], which will extend the length of the slotline. This drawback limits their applications in the antenna array.

In this paper, a novel C-band power divider is proposed. C-band (4-8 GHz) is a widely used frequency band for satellite communication [24]. Benefiting from the relationship between the coupling coefficients of the first-stage divider (microstrip-to-slotline transition (MST)) and the second-stage divider (slotline-to-microstrip transition (SMT)), both of them are self-matched respectively. Therefore, no impedance transformation is needed anymore in the slotline. It achieves 10-dB impedance bandwidth of 61.3%, from 4.3 to 8.1 GHz for any port spacing from 20 mm to 60 mm (slotline length from 28.4 mm to 68.4 mm). Then, for the first time, the microstrip-slotline coupled power divider is used to feed the Vivaldi array. The Vivaldi array could achieve 83.8% bandwidth from 3.4 to 8.3 GHz.

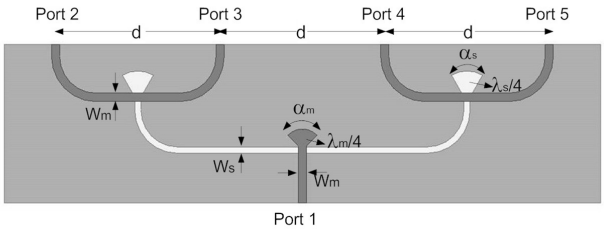

FIGURE 1. Configuration of the power divider (The dark grey color shows the front side of the substrate, while the light grey shows the bottom side).

II. THE POWER DIVIDER

The configuration of the proposed power divider is shown in Fig. 1. It is composed of one first-stage divider, i.e., MST, and two identical second-stage dividers, i.e., SMTs. In this figure, Port 1 is the input port, and the other four ports are output ports. All ports are in the form of microstrip with the characteristic impedance of 50 Ω.

In order to increase the power capacity of the power divider in MPT, a thicker substrate is preferred. Besides, from [25], We know when a specific characteristic impedance of the slotline is required, the higher the dielectric constant or the thicker the substrate, the wider the slotline width. Limited by the machining precision of the equipment in our Lab, we choose a 1.6 mm-thick Arlon AD1000 substrate with a high relative dielectric constant ε_r of 10.2, to avoid excessively narrow slotlines. Besides, the slotline has a better transmission characteristic on high dielectric constant substrates [25].

This section will be organized as follows: In Part A, the principle of the microstrip-slotline transition and its coupling coefficient are introduced. In Parts B and C, the first and second-stage power dividers are analyzed respectively. In Part D, the condition of the flexible power divider is derived. In Part E, the measured results of the prototype are given. In Part F, in order to further validate the conclusion, a narrowband flexible power divider without radial stubs is presented.

A. MICROSTRIP-SLOTLINE TRANSITION AND COUPLING COEFFICIENT

There are various types of transitions between microstrip and slotline. The simplest is the right-angle straight-line crossing [26]. However, the bandwidth is very limited. Circular stub and radial stub are two methods to expand the bandwidth. They provide wideband impedance matching and exhibit a virtual short-circuit and inductive component [27], [28]. In this paper, we use the radial stub rather than the circular stub because the radial stub could have two parameters, the flare angle and the radius. They control two aspects of the transition separately. The flare angle could adjust the coupling coefficient n. The radius controls the resonating frequency of the transition. It should be close to guided quarter wavelength.

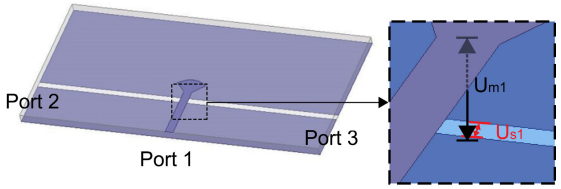

FIGURE 2. The first-stage divider.

The coupling coefficient n is usually defined as $|U_m/U_s|$, where U_m is the voltage on the microstrip line at the coupling point and U_s is that on the slotline. N. K. Das derived a closed-form expression for the coupling coefficient after making several approximations [29]. The formula is based on the crossed straight microstrip and slotline. The coupling coefficient n depends on the microstrip parameters of its width W_m and the effective dielectric constant of the substrate ε_{rem}, the slotline parameters of its width W_s and the effective dielectric constant of the substrate ε_{res}, and the height of the substrate h.

We define the coupling coefficient of MST as n_1 and that of SMT as n_2. They may be not the same because of the different structures. In the existing literature about the microstrip-slotline coupling, in [15], n_1 and n_2 are all 0.8. In [22], the exact values of n_1 and n_2 are not given; In [10], [14], [16], [30], n is not discussed, thus its value is actually assumed to be 1.

Even though N. K. Das's formula provides a clear relationship between n and its influencing factors, it cannot be applied directly in our proposed model, because of the width-varying microstrip and slotline radial stubs. Instead, we derived n from its original definition $n = |U_m/U_s|$ directly. U_m and U_s are simulated and calculated by the field calculator of ANSYS HFSS [31]. The details of the simulation process will be shown in the next two parts.

B. FIRST-STAGE DIVIDER

The first-stage divider is illustrated in Fig. 2. Port 1 is the input port. Ports 2 and 3 are output ports. The electric field is coupled and divided from the microstrip line to two opposite directions of the slotline. The end of the microstrip line is a radial stub. Its radius is approximately $\lambda_m/4$, where λ_m is the guided wavelength in microstrip of 6 GHz.

The characteristic impedance of the microstrip line Z_m is fixed at 50 Ω. Z_s is the characteristic impedance of the slotline. It is still undetermined. Then the parameter W_s, the width of the slotline, is swept by HFSS. The results are shown in Fig. 3. When W_s is 1.2 mm, corresponding to the characteristic impedance of slotline of 119 Ω at 6 GHz [32], the lowest-loss transmission is achieved.

The first-stage divider can be modeled as a transformer with the coupling coefficient n_1. n_1 is the ratio between the voltage on the microstrip line U_{m1} and that on the slotline U_{s1} at the coupling point, as shown in Fig. 2. Then we will find n_1 from the viewpoints of field and circuit respectively:

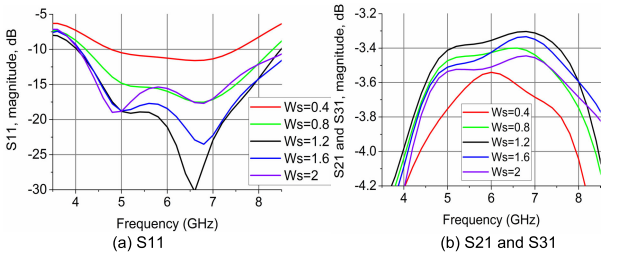

FIGURE 3. Parameter sweep of slotline width *W*s (unit: mm) for (a) S11, (b) S21 and S31 in the first-stage divider.

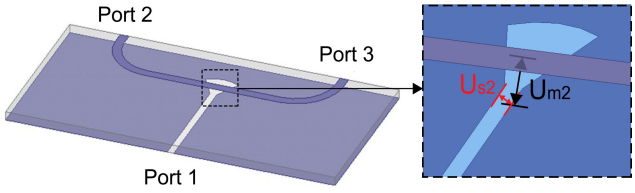

FIGURE 4. The second-stage divider.

1) FROM THE VIEWPOINT OF FIELD

The input power at Port 1 is set to 0 dBm. Then the field distribution is simulated by the field calculator of HFSS. At the coupling point, the maximum value of microstrip voltage $|U_{m1}|$ is 0.327 V and that of slotline $|U_{s1}|$ is 0.345 V. So,

$$n_1 = \frac{|U_{m1}|}{|U_{s1}|} = 0.95 \tag{1}$$

2) FROM THE VIEWPOINT OF CIRCUIT

We assume in this condition the power divider is lossless, which means the input power equals to the total output power, so,

$$\frac{1}{2}\frac{|U_{m1}|^2}{Z_m} = P_{in} = P_{out} = 2 \times \frac{1}{2}\frac{|U_{s1}|^2}{Z_s} \tag{2}$$

Then

$$\frac{Z_m}{Z_s} = \frac{n_1^2}{2} \tag{3}$$

According to (3), in this implementation and at the center frequency 6 GHz, for $Z_m = 50\Omega$ and $Z_s = 119\Omega$. It is calculated that $n_1 = 0.92$.

As can be seen, the two values of n_1 calculated from the field and the circuit are close.

C. SECOND-STAGE DIVIDER

There are two identical second-stage dividers, as shown in Fig. 4. Port 1 is the input port, whereas Ports 2 and 3 are output ports. The end of the slotline is a radial stub, with flare angle α_s. The radius is about $\lambda_s/4$, where λ_s is the guided wavelength in slotline of 6 GHz. The whole stub exhibits a virtual open-circuit and capacitance [27]. Due to the opposite directions of the electric field when it is divided to the two arms of the microstrip line, the two output ports

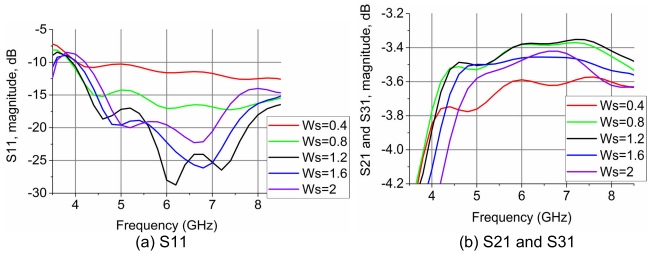

FIGURE 5. Parameter sweep of slotline width *Ws* (unit: mm) for (a) S11, (b) S21 and S31 in the second-stage divider.

of the second-stage divider are in equal magnitude but 180° phase difference [22].

Z_m of the microstrip line is fixed at 50 Ω. The flare angle of the radial slot stub could be tuned to change n_2. The width of slotline W_s is swept in HFSS, as shown in Fig. 5. When W_s is 1.2 mm, corresponding to a characteristic impedance of 119 Ω at 6 GHz [32], the lowest-loss transmission is achieved. Then we can find n_2:

1) FROM THE VIEWPOINT OF FIELD

U_{m2} is the voltage on microstrip at the coupling point, whereas U_{s2} is that on slotline, as shown in Fig. 4. The input power is set to 0 dBm. In HFSS, $|U_{m2}|$ is calculated as 0.260 V and $|U_{s2}|$ is 0.461 V. So,

$$n_2 = \frac{|U_{m2}|}{|U_{s2}|} = 0.56 \tag{4}$$

2) FROM THE VIEWPOINT OF CIRCUIT

On the other hand, we assume in this condition the power divider is lossless. So,

$$\frac{1}{2}\frac{|U_{s2}|^2}{Z_s} = P_{in} = P_{out} = 2 \times \frac{1}{2}\frac{|U_{m2}|^2}{Z_m} \tag{5}$$

Thus,

$$\frac{Z_m}{Z_s} = 2n_2^2 \tag{6}$$

According to (6), $Z_m = 50\Omega$ and $Z_s = 119\Omega$. So, $n_2 = 0.44$.

The discrepancy between the two values of n_2 calculated from the field and the circuit may be from the ideal hypothesis of lossless power, and the simulation precision.

D. CONDITION OF FLEXIBLE POWER DIVIDER

All from the viewpoint of the circuit, we can combine (3) and (6). Then,

$$\frac{Z_m}{Z_s} = \frac{n_1^2}{2} = 2n_2^2 \tag{7}$$

$$\frac{n_1}{n_2} = 2 \tag{8}$$

It indicates that for this MSM power divider with standard 50 Ω ports and invariable slotline width. if $n_1/n_2 = 2$, the first-stage and second-stage dividers will be self-matched

TABLE 3. Dimensions of the proposed power divider.

W_m	W_s	$\lambda_s/4$	$\lambda_m/4$	α_s	α_m
1.6 mm	1.2 mm	6 mm	4 mm	60°	90°

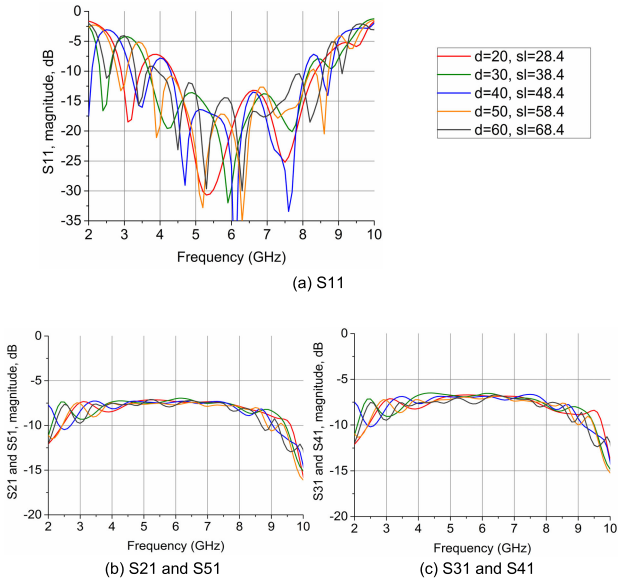

FIGURE 6. Simulated reflection and transmission coefficients versus port spacing *d* and the slot length *sl* (unit: mm).

respectively. Then no impedance matching is needed anymore in the slotline.

From the simulation result of Sections II(B) and II(C), the detailed dimensions of the proposed power divider are shown in Table 3.

Fig. 6 shows the simulated reflection and transmission coefficient of the power divider. The output port spacing d(corresponding to the slotline length sl between the first and second-stage dividers) varies when all other parameters keep unchanged. In the frequency band of 4.3-8.1 GHz (61.3% bandwidth), for d from 20 mm to 60 mm (corresponding respectively to 0.4λ and 1.2λ of 6 GHz), the reflection coefficient is lower than −10 dB. Compared with other microstrip-slotline coupled power dividers, the flare angles of the proposed power divider should be tuned in order to satisfy $n_1/n_2 = 2$, instead of pursuing the widest bandwidth. So, further expansion of the bandwidth will be impeded. Ports 2 and 5 have an insertion loss of 7.5 dB ± 0.5 dB. Ports 3 and 4 have the insertion loss of 7 dB ± 0.5 dB. The same MSM four-way power dividers exhibit the insertion loss of 6.8 ± 0.4 dB [22] and 8 dB [23]. The higher insertion loss may come from the surface wave because the substrate has a high dielectric constant and large thickness.

E. PROTOTYPE AND MEASUREMENT

Then a prototype with $d = 32$ mm is fabricated for further development of the antenna array, as shown in Fig. 7. The simulated and measured reflection and transmission

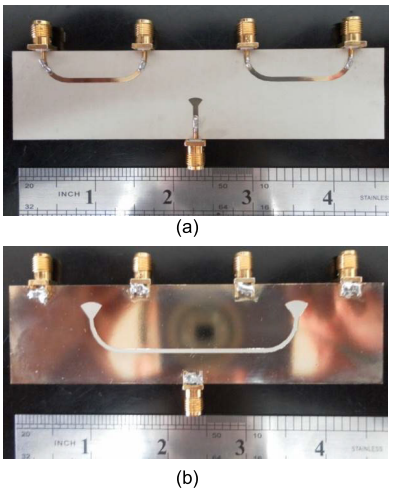

FIGURE 7. Prototype of the proposed power divider: (a) the top view, (b) the bottom view.

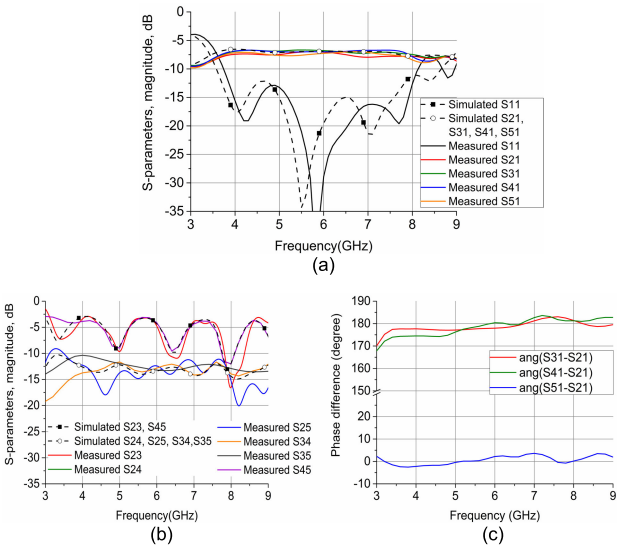

FIGURE 8. Simulated and measured (a) reflection and transmission coefficients, (b) isolations, and (c) measured phase differences of the four output ports.

coefficients are shown in Fig. 8(a). In the frequency band of 3.8-8.1 GHz, the measured reflection coefficient is lower than -10 dB. The isolations of the four output ports are shown in Fig. 8(b): S_{24}, S_{25}, S_{34}, and S_{35} are lower than -10 dB. S_{23} and S_{45} are within -9.3 ± 6.4 dB because of the directly connected microstrip output ports. Considering that this power divider is used for microwave power transmission instead of communication, we did not take special measures to improve the isolation. The phase responses of the output ports are shown in Fig. 8(c). As expected, Ports 3 and 4 have a 180° phase difference with Ports 2 and 5.

F. NARROWBAND ARBITRARY PORT-SPACING POWER DIVIDER WITHOUT RADIAL STUBS

The microstrip and slotline radial stubs could expand the bandwidth of the power divider [27], comparing with the

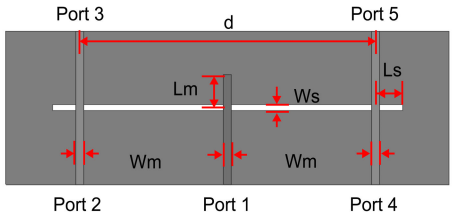

FIGURE 9. Narrowband power divider without radial stubs ($W_m = 1.6$ mm, $W_s = 1.2$ mm, $L_s = 5.5$ mm, $L_m = 6.5$ mm).

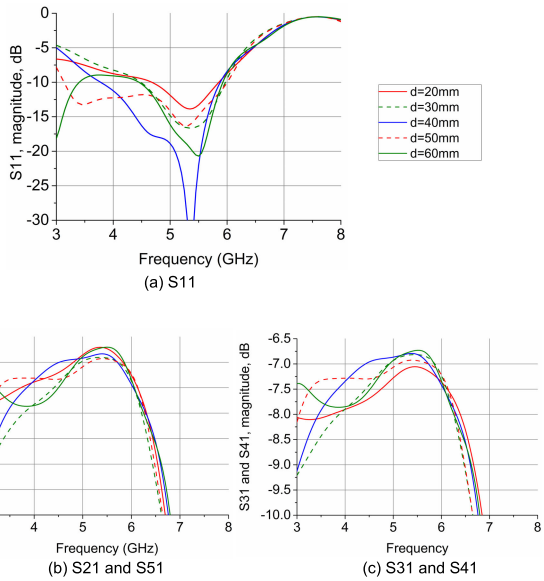

FIGURE 10. Simulated reflection and transmission coefficient of narrowband power divider versus port spacing d.

straight line crossing [28]. The flare angles α_m and α_s could adjust the coupling coefficient n_1 and n_2 respectively more easily. However, it is noteworthy that the radial stubs are not the essential reason and necessary condition of the self-matching. The essential reason is the relationship of $n_1/n_2 = 2$. To validate it, we further exhibit a narrow-band power divider without radial stubs, as shown in Fig. 9. It is on the same substrate with the previous wideband one. The simulated reflection and transmission coefficients versus port spacing d are shown in Fig. 10.

As shown in the simulation, for this power divider, the length of the slotline has very small impact.

III. VIVALDI ANTENNA ARRAY

Furthermore, a Vivaldi antenna array is developed by using the proposed power divider. The detailed data of the Vivaldi antenna element is shown in Fig. 11 and Table 4. The prototype of the antenna array is shown in Fig. 12. The antenna elements are aligned in H-plane. Since the target operating frequency band is 4-8 GHz, the element spacing is chosen as 32 mm, corresponding to $0.64\lambda_0$ (λ_0 is the free space wavelength of the central frequency). Since the phase shifts at four output ports of the power divider are 0°, 180°, 180°, and 0°,

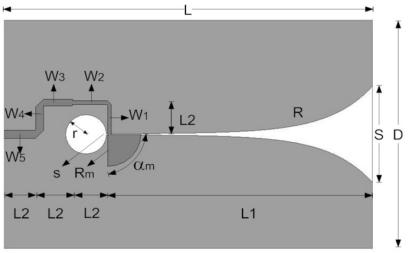

FIGURE 11. Configuration of the Vivaldi antenna element.

TABLE 4. Details of Vivaldi antenna element (Substrates: Rogers Duroid 4003C, $h = 0.8$ mm, $\varepsilon_r = 3.38$, tan $\delta = 0.002$).

L	L_1	L_2	D	S	W_1	W_2	W_3
77.4 mm	55.2 mm	7.4 mm	50 mm	21 mm	0.7 mm	0.9 mm	1.4 mm
W_4	W_5	s	R	R_m	r	α_m	
1.7 mm	1.8 mm	0.3 mm	0.11	7 mm	4.3 mm	83°	

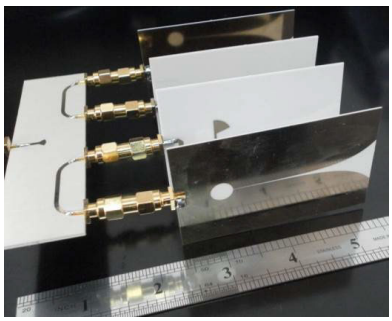

FIGURE 12. Prototype of the Vivaldi antenna array.

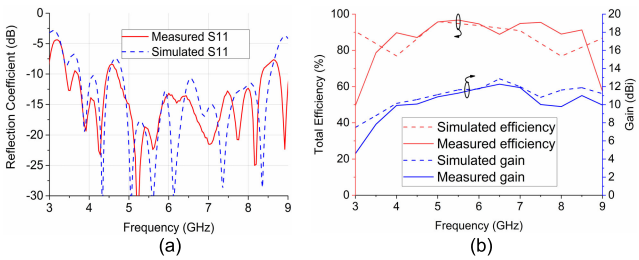

FIGURE 13. Simulated and measured (a) reflection coefficient and (b) broadside peak gain versus frequency.

the four elements are placed positively, negatively, negatively and positively in order.

The simulated and measured reflection coefficients of the antenna array are shown in Fig. 13(a). The impedance bandwidth of the array is 3.4–8.3 GHz, except for 4.6 GHz lower than −8.4 dB, corresponding to an 83.8% bandwidth. Fig. 13(b) shows the simulated and measured broadside peak gain of the 1×4 array. The measured maximum gain of the array is 12.6 dBi at 6 GHz. When deviating from the central frequency, the maximum gain is decreased. It is because of the decreased gain of the Vivaldi antenna element and the

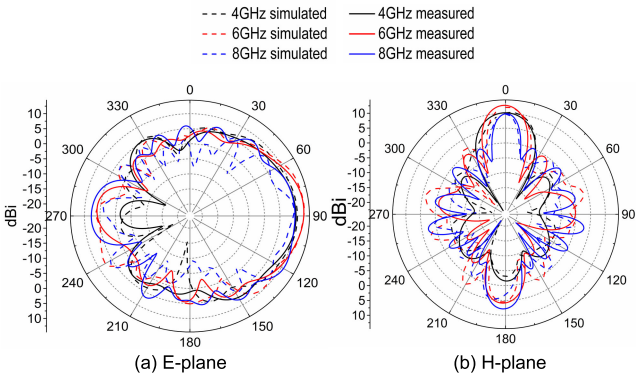

FIGURE 14. Simulated and measured radiation patterns of the antenna array at 4 GHz, 6 GHz, and 8 GHz in (a) E-plane and (b) H-plane.

increased insertion loss of the feed network when deviating from the central frequency. But in the operating frequency band, the gain is higher than 9 dBi. Fig. 14 shows the simulated and measured E-plane and H-plane radiation patterns of the antenna array at 4 GHz, 6 GHz, and 8 GHz. The back lobe may result from the surface wave produced by the thick and high-dielectric-constant substrate of the power divider. In short, the antenna array performs wideband property when it is fed by the proposed power divider.

IV. CONCLUSION

In this paper, a flexible power divider is presented for the feed network of wideband antenna array. When the two coupling coefficients of MST and SMT $n_1/n_2 = 2$, the first and second stages are self-matched respectively. Then, no impedance transformation is needed anymore in the slotline. It eliminates the drawback limiting the free wire routing of the feed network. Especially, it could be considered when simple T-junction feed networks cannot achieve enough bandwidth.

REFERENCES

[1] N. Shinohara and H. Matsumoto, "Experimental study of large rectenna array for microwave energy transmission," *IEEE Trans. Microw. Theory Techn.*, vol. 46, no. 3, pp. 261–268, Mar. 1998.
[2] P. J. Gibson, "The vivaldi aerial," in *Proc. 9th Eur. Microw. Conf.*, Sep. 1979, pp. 101–105.
[3] R. Janaswamy and D. Schaubert, "Analysis of the tapered slot antenna," *IEEE Trans. Antennas Propag.*, vol. 35, no. 9, pp. 1058–1065, Sep. 1987.
[4] S. Oh, S. Seo, M. Yoon, C. Oh, E. Kim, and Y. Kim, "A broadband microstrip antenna array for LMDS applications," *Microw. Opt. Technol. Lett.*, vol. 32, no. 1, pp. 35–37, Jan. 2002.
[5] H. Wang, X. Huang, and D.-G. Fang, "A single layer wideband U-slot microstrip patch antenna array," *IEEE Antennas Wireless Propag. Lett.*, vol. 7, pp. 9–12, 2008.
[6] H. Wang, D.-G. Fang, and X. G. Chen, "A compact single layer monopulse microstrip antenna array," *IEEE Trans. Antennas Propag.*, vol. 54, no. 2, pp. 503–509, Feb. 2006.
[7] G. Brzezina, R. E. Amaya, A. Petosa, and L. Roy, "Broadband and compact Vivaldi arrays in LTCC for 60 GHz point-to-point networks," in *Proc. WAMICON*, Jun. 2014, pp. 1–5.
[8] H. Wong, K.-L. Lau, and K.-M. Luk, "Design of dual-polarized L-probe patch antenna arrays with high isolation," *IEEE Trans. Antennas Propag.*, vol. 52, no. 1, pp. 45–52, Jan. 2004.

[9] S. W. Wong and L. Zhu, "Ultra-wideband power divider with good in-band splitting and isolation performances," *IEEE Microw. Wireless Compon. Lett.*, vol. 18, no. 8, pp. 518–520, Aug. 2008.
[10] U. T. Ahmed and A. M. Abbosh, "Modified Wilkinson power divider using coupled microstrip lines and shunt open-ended stubs," *Electron. Lett.*, vol. 51, no. 11, pp. 838–839, May 2015.
[11] Y. Yao and Z. Feng, "A band-notched ultra-wideband 1 to 4 Wilkinson power divider using symmetric defected ground structure," in *Proc. IEEE Antennas Propag. Soc. Int. Symp.*, Jun. 2007, pp. 1557–1560.
[12] Y. Yang, C. Zhang, S. Lin, and A. E. Fathy, "Development of an ultra wideband Vivaldi antenna array," in *Proc. IEEE Antennas Propag. Soc. Int. Symp.*, vol. 1, Jul. 2005, pp. 606–609.
[13] Y. Yao, M. Liu, W. Chen, and Z. Feng, "Analysis and design of wideband widescan planar tapered slot antenna array," *IET Microw., Antennas Propag.*, vol. 4, no. 10, pp. 1632–1638, Oct. 2010.
[14] K. Song and Q. Xue, "Novel ultra-wideband (UWB) multilayer slotline power divider with bandpass response," *IEEE Microw. Wireless Compon. Lett.*, vol. 20, no. 1, pp. 13–15, Jan. 2010.
[15] M. E. Bialkowski and A. M. Abbosh, "Design of a compact UWB out-of-phase power divider," *IEEE Microw. Wireless Compon. Lett.*, vol. 17, no. 4, pp. 289–291, Apr. 2007.
[16] N. Seman, M. E. Bialkowski, and W. C. Khor, "Ultra wideband vias and power dividers in microstrip-slot technology," in *Proc. Asia–Pacific Microw. Conf.*, Dec. 2007, pp. 1–4.
[17] K. Song and Q. Xue, "Ultra-wideband out-of-phase power divider using multilayer microstrip-slotline coupling structure," *Microw. Opt. Technol. Lett.*, vol. 52, no. 7, pp. 1591–1594, Jul. 2010.
[18] H. Ogawa, T. Hirota, and M. Aikawa, "New MIC power dividers using coupled microstrip-slot lines: Two-sided MIC power dividers," *IEEE Trans. Microw. Theory Techn.*, vol. MTT-33, no. 11, pp. 1155–1164, Nov. 1985.
[19] J. S. Kim, M. J. Park, and M. G. Kim, "Out-of-phase Wilkinson power divider," *Electron. Lett.*, vol. 45, no. 1, pp. 59–60, Jan. 2009.
[20] L. Guo, A. Abbosh, and H. Zhu, "Ultra-wideband in-phase power divider using stepped-impedance three-line coupled structure and microstrip-to-slotline transitions," *Electron. Lett.*, vol. 50, no. 5, pp. 383–384, Feb. 2014.
[21] U. T. Ahmed and A. M. Abbosh, "Wideband out-of-phase power divider using tightly coupled lines and microstrip to slotline transitions," *Electron. Lett.*, vol. 52, no. 2, pp. 126–128, 2016.
[22] K. Song, Y. Mo, Q. Xue, and Y. Fan, "Wideband four-way out-of-phase slotline power dividers," *IEEE Trans. Ind. Electron.*, vol. 61, no. 7, pp. 3598–3606, Jul. 2014.
[23] B. Xiao, J.-S. Hong, and B.-Z. Wang, "A novel UWB out-of-phase four-way power divider," *Appl. Comput. Electromagn. Soc. J.*, vol. 26, no. 10, p. 863, Oct. 2011.
[24] A. K. Maini and V. Agrawal, *Satellite Technology: Principles and Applications*, 3rd ed. Hoboken, NJ, USA: Wiley, 2011.
[25] S. B. Cohn, "Slot line on a dielectric substrate," *IEEE Trans. Microw. Theory Techn.*, vol. 17, no. 10, pp. 768–778, Oct. 1969.
[26] R. Garg, I. Bahl, and M. Bozzi, *Microstrip Lines and Slotlines*, 3rd ed. Norwood, MA, USA: Artech House, 2013.
[27] M. M. Zinieris, R. Sloan, and L. E. Davis, "A broadband microstrip-to-slotline transition," *Microw. Opt. Technol. Lett.*, vol. 18, no. 5, pp. 339–342, Aug. 1998.
[28] B. Shuppert, "Microstrip/slotline transitions: Modeling and experimental investigation," *IEEE Trans. Microw. Theory Techn.*, vol. 36, no. 8, pp. 1272–1282, Aug. 1988.
[29] N. K. Das, "Generalized multiport reciprocity analysis of surface-to-surface transitions between multiple printed transmission lines," *IEEE Trans. Microw. Theory Techn.*, vol. 41, no. 6, pp. 1164–1177, Jun. 1993.
[30] R. Li and L. Zhu, "Ultra-Wideband (UWB) Bandpass Filters With Hybrid Microstrip/Slotline Structures," *IEEE Microw. Wireless Compon. Lett.*, vol. 17, no. 11, pp. 778–780, Nov. 2007.
[31] *ANSYS HFSS: High Frequency Electromagnetic Field Simulation Software*. Accessed: Mar. 27, 2019. [Online]. Available: https://www.ansys.com/products/electronics/ansys-hfss
[32] E. A. Mariani, C. P. Heinzman, J. P. Agrios, and S. B. Cohn, "Slot line characteristics," *IEEE Trans. Microw. Theory Techn.*, vol. MIT-17, no. 12, pp. 1091–1096, Dec. 1969.

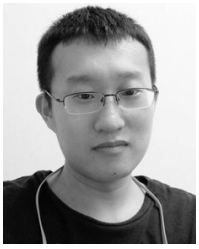

BING XIAO received the B.Sc. degree in applied physics from Anhui University, Hefei, China, in 2009, and the M.Sc. degree in radio physics from the University of Electronic Science and Technology of China (UESTC), Chengdu, China, in 2012. He is currently pursuing the Ph.D. degree in electronic engineering with The University of Hong Kong, Hong Kong. He started his career as an Antenna/RF Engineer in 2012, with the China Electronics Technology Group Corporation (CETC) and then Xiaomi Corporation. His current research interests include antennas of smart devices and the IoT.

HEMING YAO received the B.S. degree in information and computing science and the M.S. degree in electronic and communication engineering from Beihang University, Beijing, China, in 2013 and 2016, respectively. He is currently pursuing the Ph.D. degree with the Department of Electrical and Electronic Engineering, The University of Hong Kong, Hong Kong. His research interests include EMC/EMI, machine learning, and advanced materials.

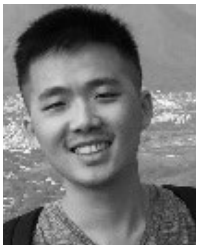

MIN LI (S'14–M'18) received the B.S. degree from UESTC, Chengdu, China, in 2014, and the Ph.D. degree from The University of Hong Kong, Hong Kong, in 2018, where he is currently a Postdoctoral Researcher with the Department of Electrical and Electronic Engineering. His current research interests include antenna design and multiple-input multiple-output antenna decoupling.

JING-SONG HONG received the B.Sc. degree in electromagnetics from Lanzhou University, China, in 1991, and the M.Sc. and Ph. D. degrees in electrical engineering from the University of Electronic Science and Technology of China (UESTC), in 2000 and 2005, respectively. From 1991 to 1993, he was a Circuit Designer with the Jingjiang Radar Factory, Chengdu, China. From 1993 to 1997, he was a Testing Engineer with SAE Magnetics (HK) Ltd., Guangdong, China. From 1999 to 2002, he was a Research Assistant with the City University of Hong Kong. He is currently a Professor with UESTC. His research interests include the use of numerical techniques in electromagnetics, and the use of microwave methods for materials characterization and processing.

KWAN L. YEUNG (S'93–M'95–SM'99) was born in 1969. He received the B.Eng. and Ph.D. degrees in information engineering from The Chinese University of Hong Kong, in 1992 and 1995, respectively. He joined the Department of Electrical and Electronic Engineering, The University of Hong Kong, in July 2000, where he is currently a Professor. His research interests include the next-generation Internet, packet switch/router design, all-optical networks, and wireless data networks.